Design and Simulation of Low Pass and Band Stop Microwave Filters

Talal Altaher Ahmed Mohammed [1] [*], Ahmed lmhmed Salim Elstia [2], Abdulghader Basher Morad Jalgum [3], Ibrahem Mohamed Ibrahem Abdaldaem [4]

[1,2] Department of Electrical and Electronic Technologies, Higher Institute of Sciences and Technology Tamzawah, Tamzawah Alshati, Libya

[3] Department of Information Technology, College of Sciences and Technology Alzweah, Alzweah Alshati, Libya

[4] Department of Electrical and Electronic Technologies, Higher Institute of Sciences and Technology Aljufra, Sukna, Libya

تصميم ومحاكاة مرشحات الموجات الدقيقة ذات الترددات المنخفضة وترددات إيقاف النطاق

طلال الطاهر أحمد محمد[1]*، أحمد إمحمد سالم السطيل[2]، عبد القادر بشير مراد جلغم[3]، إبراهيم محمد إبراهيم عبد الدائم[4]

[1,2] قسم التقنيات الكهربائية والإلكترونية، المعهد العالي للعلوم والتقنية تامزاوة، تامزاوة الشاطئ، ليبيا

[3] قسم تقنية المعلومات، كلية العلوم والتقنية الزوية، الزوية الشاطئ، ليبيا

[4] قسم التقنيات الكهربائية والإلكترونية، المعهد العالي للعلوم والتقنية الجفرة، سوكنة، ليبيا

[*]Corresponding author: Gigma1986@gmail.com

Abstract:

The design & simulation of microwave filters such as fifth order Low Pass Filter (LPF) and Band-Stop Filter (BSF) with maximally flat (Butterworth) response is presented in this paper. The two filters were initially designed using lumped-element (LC) method. Additionally, they tested this LPF as a stepped impedance microstrip line for real-life applications as distributed element. All designs and simulations took place on Advanced Design System (ADS) software. According to simulation results, the lumped-element LPF has a cutoff frequency of 2 GHz and offers high passband rejection of 54 dB at stopband frequency of 7 GHz. The stepped impedance microstrip LPF has the same cutoff of 2 GHz and a similar filter response. Thus, there is a fair comparison between the two implementation techniques. The simulated response of the lumped-element BSF also confirms a well-defined stopband behavior from 3 GHz to 7 GHz, thereby satisfying the desired design specifications.

Keywords: Microwave fitters, Low pass filter, Band stop filter, Microstrip line

الملخص

تُقدَّم هذه الورقة تصميم ومحاكاة مرشحات الموجات الدقيقة مثل مرشح تمرير الترددات المنخفضة (LPF) من الدرجة الخامسة ومرشح إيقاف النطاق (BSF)، باستجابة مسطحة قصوى (Butterworth). صُمِّم المرشحان في البداية باستخدام طريقة العناصر المُجمعة (LC). بالإضافة إلى ذلك، تم اختبار مرشح تمرير الترددات المنخفضة كخط شريطي دقيق ذي معاوقة متدرجة لتطبيقات العملية كعنصر موزع. أُجريت جميع التصميمات والمحاكاة باستخدام برنامج نظام التصميم المتقدم (ADS). ووفقًا لنتائج المحاكاة، فإن مرشح تمرير الترددات المنخفضة ذو العناصر المُجمعة له تردد قطع يبلغ 2 جيجاهرتز، ويوفر رفضًا عاليًا لنطاق التمرير يبلغ 54 ديسيبل عند تردد نطاق التوقف البالغ 7 جيجاهرتز. أما مرشح تمرير الترددات المنخفضة ذو المعاوقة المتدرجة، فله نفس تردد القطع البالغ 2 جيجاهرتز، واستجابة مرشح مماثلة. وبالتالي، تُوجد مقارنة

عادلة بين تقنيتي التنفيذ. كما تؤكد استجابة المحاكاة لمرشح إيقاف النطاق ذو العناصر المُجمعة سلوكًا واضحًا لنطاق التوقف من 3 جيجاهرتز إلى 7 جيجاهرتز، مما يُلبي مواصفات التصميم المطلوبة.

الكلمات المفتاحية: مُرشحات الميكروويف، مرشح الترددات المنخفضة، مرشح إيقاف النطاق، الخط الشريطي الدقيق.

Introduction

Microwave filters are one of microwave passive components that play a major role to control the frequency at certain point in various communications systems, particularly communications satellites, earth stations, wireless base stations, and repeaters (Cao et al., 2025). They are two-port networks aimed at providing transmission at frequencies within the passband of the filter and attenuation in the stopband of the filter. There are many types of filters, and all of them widely used according to the needs of different applications (Amini et al., 2024). Generally, filters are categorized based on their frequency selection or by their function response [1-2,].

Based of frequency selection filters can be low pass filter (LPF), high pass filter (HPF), band pass filter (BPF) or band stop filter (BSF). The low pass and high pass characteristics have the cutoff frequency, defined by the specified insertion loss in decibels, at which the passband ends (Dobrev et al., 2025).

The LPF transfers energy to the load at frequencies lower than the cutoff frequency with minimal attenuation and reflects an increasing fraction of the energy back to the sources the frequency is increased above the cutoff frequency. The HPF transfers energy to the load at frequencies higher than the cutoff frequency with minimal attenuation and reflects an increasing fraction of the energy back to the source as the frequency is decreased below the cutoff frequency. On the other hand, the band pass and band stop filter characteristics have two cutoff frequencies, or band-edge frequencies, which are defined by the specified insertion loss in decibels. In the BPF, energy is transferred to the load in a band of frequencies between the lower and upper cutoff frequencies. In the BSF energy transfers to the load in two frequency bands: from dc to the lower band stop cutoff and from the upper band stop cutoff to infinite frequency (Xiao et al., 2025).

According to function response, the most popular filters are maximally flat response (Binomial or Butterworth), equal ripple response (Chebyshev). Butterworth of binomial response function filter is characterized by no ripples in the pass band frequencies, and their insertion loss is flat and rises monotonously with changing frequency in the frequency band. Thus, the popular name is maximally flat response filters (Zhang et al., 2025). In contrast, a Chebyshev response function filter has equal replies in the passband, and it provides the sharpest possible rise of the insertion loss with frequency for a maximum specified passband insertion loss ripple. Besides that, there are elliptic function response and liner phase response filters. Elliptic function response filters have equal ripple response in the pass band as well as the stop band frequency range. Filters can also have liner phase response as required in some applications to avoid signal distortion (Wu et al., 2024).

In this paper, designed and simulation of low pass filter (LPF) and band stop filter (BSF) will be presented. Both filters are designed using lamped elements (L and C) with maximally flat function response. In addition, LPF is also designed using step impedance microstrip line method.

The following sections of this paper are organized as; section I is filter design procedure, while section III contains the simulation results and discussion. Lastly, summary conclusion for what has been done and the achievement in this paper is highlighted in section IV.

Filter Design Procedure

The section is mainly highlighted the steps that needs to be followed in order to design the desired filter. Basically, any design has specification that must be known and taken in consideration. Mainly for filters, type of filter, filter function response has to be known (Selvaprasanth et al., 2025). There are some other specifications that need to be specified as cutoff frequency, attenuation level to obtain the number of orders (L and C elements) (Liu et al., 2025).

A. Low Pass Filter (LPF) Design Steps

Step.1: Design specification

The low pass filter (LPF) that need to be designed has cutoff frequency (f_c) at 2GHz, and attenuation of 50 dB at frequency (f) 7GHz. Moreover, LPF response is maximally flat.

Step.2: Obtain the number of orders N he number of orders can be obtained as following [1]:

$$\left|\frac{\omega}{\omega_c}\right| - 1 \qquad (1)$$

Where $\omega_c = 2\pi f_c$, while $\omega = 2\pi f$

By using the obtained value from equation (1) and attenuation level for desired LPF, the number of orders lamped elements for LPF prototype can be gotten using maximally flat LPF graph at (Liu et al., 2025). In this design, number of orders N=5.

Step.3: Prototype element value

For maximally flat (Butterworth) LPF prototype element value is obtained from presented data for N=5 is listed in Table 1.

Step.4: Scaling and conversion (Transformation)

In order to design actual low pass filters, the transformations of the low pass prototype filters with cut-off frequency, $\omega_c = 2\,GHz$ and having the source resistance $R_s = 50\,\Omega$ and load resistances R_L are made into the desired. The values of lamped elements are calculated using scaling equations as following (Liu et al., 2025):

$$C = \frac{g_K R}{\omega_C} \qquad (2)$$

$$L = \frac{g_k}{\omega_C R} \qquad (3)$$

$$R_L = R_S \times g_{N+1} \qquad (4)$$

Figure 1 shows maximally flat LPF circuit m while table1 contains the prototype element values and corresponding L and C elements value.
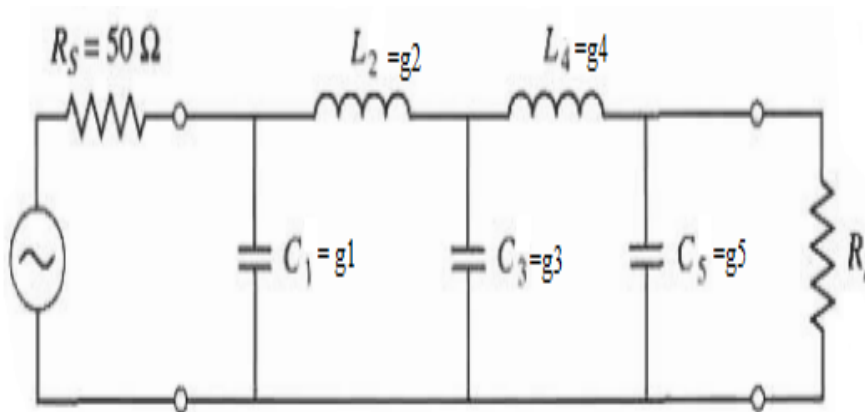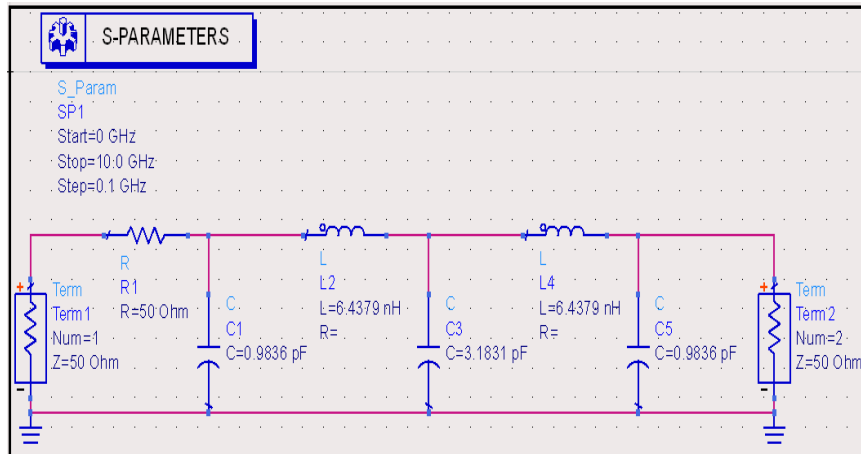

Figure 1. Low pass, maximally flat filter circuit

Table1. Prototype element and corresponding lamped elements value.

Prototype Elements (N=5)	g_1	g_2	g_3	g_4	g_5	g_6
	0.06180	1.6180	2.0000	1.6180	0.6180	1.0000
Lumped Elements	C1()	L2(nH)	C3(pF)	L4(nH)	C5(pF)	R_L
	0.9836	6.4397	3.1831	6.437	0.9836	50 Ω

ADS schematic diagram for LPF using lamped elements is show in Figure2.

Figure 2. ADS schematic diagram for LPF

B. Design LPF using Microstrip line Step-impedance

Microstrip line is an easy and another way to design and implement LPF. It is mainly microstrip sections of vary high and very low characteristics impedance lines. This type of filter called LPF stepped-impedance (Romero et al., 2025). As has been illustrated, the designed LPF in this paper has five lamped elements (N=5), thus, the equivalent LPF stepped impedance has five microstrip line sections as shown in Figure 3. The electric length of inductor (L) and capacitor (C) sections can be calculated as (Modaberi et al., 2025):

$$\beta_l = \frac{g_K R_0}{Z_h} \ (inductor) \tag{5}$$

$$\beta_l = \frac{g_K Z_l}{R_0} \ (capacitor) \tag{6}$$

Where $Z_h = 120\Omega$, $Z_l = 20\Omega$ and $R_0 = 50\Omega$
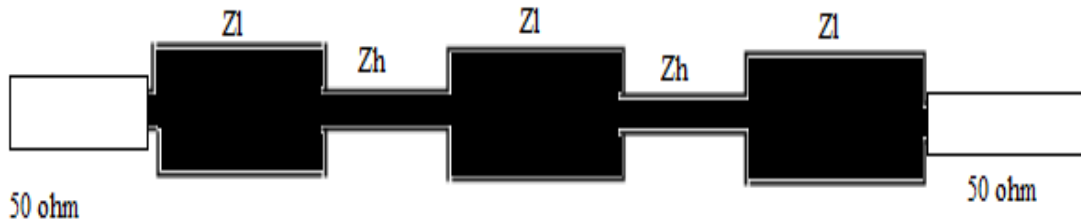
Figure 3. LPF microstrip line step-impedance circuit

Specifications of microstrip line that used to design LPF step-impedance are included in Table 2:

**Table 2.** Microstrip line specification

Parameters	Values
Substrate Dielectric Constant (ε_r)	4.50
Substrate thickness (h)	0.508 mm
S Loss tangent (tan δ)	0.0020
M Metallization	17μm copper
N Filter response	Maximally flat

Determines of the microstrip line sections are determined using ADS LineCalc tool and listed in table3. These dimensions of each section obtained at its corresponding electric length and its characteristic impedance.

Table 3. LPF microstrip step-impedance dimensions.

Section number	Sections Impedance (Ω)	Element Prototype (g_K)	Electric Length (degree)	Section Dimension (mm)	
				L	W
1	$Z_l = 20$	0.6180	14.16^o	3.018	3.46
2	$Z_h = 120$	1.6180	38.63^o	9.448	0.106
3	$Z_l = 20$	2.0000	45.84^o	9.767	3.461
4	$Z_h = 120$	1.6180	38.63^o	9.448	0.106
5	$Z_l = 20$	0.6180	14.16^o	3.018	3.46

Based on the parameters that has calculated and listed in table 1, ADS Schematic for LPF strip-impedance and its layout are shown in Figure 4 and Figure 5 respectively.
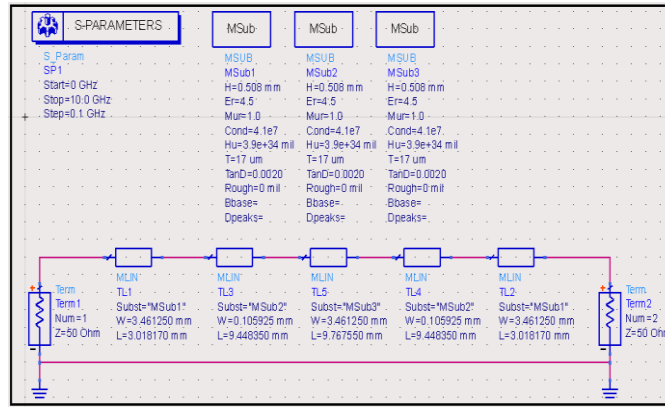
Figure 4. ADS schematic for step-impedance LPF.
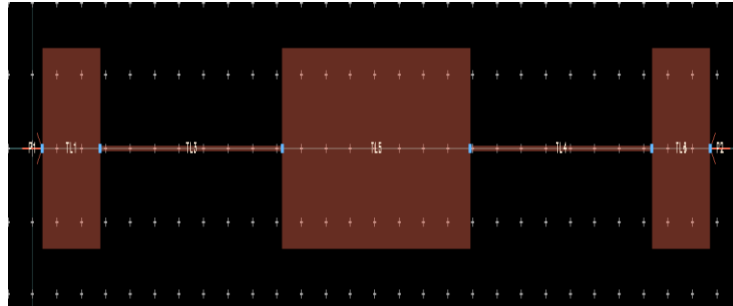
Figure 5. Layout of step-impedance LPF

A. Band stop filter (BSF) Design steps

Design procedures for band stop filter (BSF) are the same once that used to design LPF. The only deferent is in the scaling step in which the capacitors are replaced with serial of L and C lamped element while the inductors are replaced by parallel L and C lamped elements (Li et al., 2025). The number of order N=5 and the element value prototype of BSF equal to the once obtain for LPF. In addition, BSF need to have stopband range from 3 to 7 GHz. For serial lamped elements, the values of L and C can be calculated using equations as following (Modaberi et al., 2025):

$$C = \frac{g_k \, \Delta}{\omega_0 R} \tag{7}$$

$$L = \frac{R}{\omega_0 \, g_K \, \Delta} \tag{8}$$

For the parallel lamped elements, the values of L and C can be calculated using equations as following:

$$C = \frac{1}{\omega_0 R \, g_k \, \Delta} \tag{9}$$

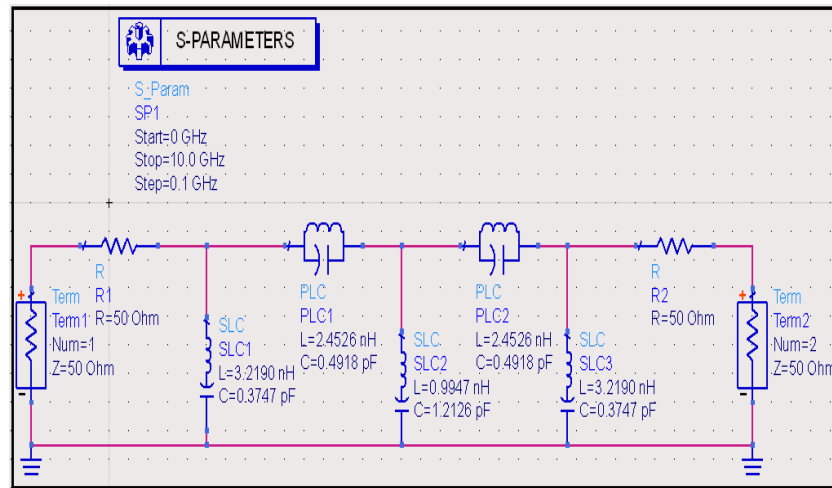$$L = \frac{g_K \Delta R}{\omega_o} \quad (10)$$

Where:

$$\omega_o = \sqrt{\omega_1 \times \omega_2} \quad (11)$$

$$\Delta = \frac{\omega_1 - \omega_2}{\omega_o} \quad (12)$$

**Table 4.** Prototype corresponding lamped elements value for BSF

Prototype Elements (N=5)	g_1	g_2	g_3	g_4	g_5	g_6
	0.6180	1.6180	2.0000	1.618	0.6180	1.0000
Lumped Elements	L1(nH)	C2	C3	C4	C5	R_L
	0.3747	0.4918	1.2126	0.4918	0.3747	50Ω
	L1(nH)	L2(nH)	L3(nH)	L4(nH)	L5(nH)	R_L
	3.2190	2.4526	0.9947	2.4526	3.2190	50Ω

Figure 6. ADS schematic diagram for BSF

Simulation Results and Discussion

As has been mentioned, all designed filters are simulated using ADS software. The simulation results are mainly filter response curves that illustrate the relation between the attenuation level and frequencies. For the lamped element LPF, the simulation result is shown in Figure 7.
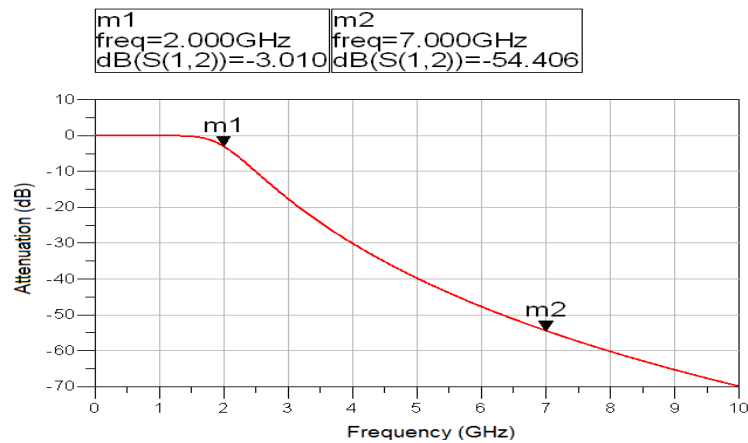
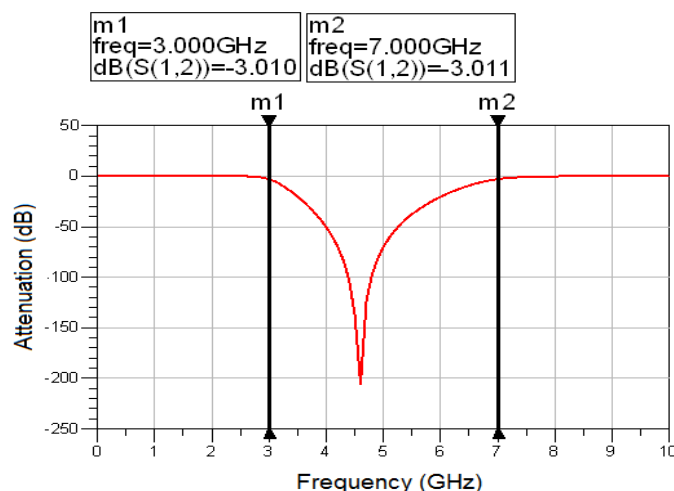**Figure 7.** Response of lamped element LPF.

As can be seen in Figure 7, insertion loss curve (blue line) indicates that LPF has cutoff frequency at 2GHz. Thus, the LPF allows passing the frequencies less than 2GHz and rejects those frequencies more than that. Also, LPF has attenuation level of equal to -54dB at 7GHz; which is close to the desired attenuation level (50dB).

The response for step—impedance LPF is also plotted and shown in Figure8. As it observed, LPF with microstrip line step-impedance still maintain the same cutoff frequency 2GHz as lamped element LPF. But the amount of attenuation level that required to be at 7GHz is completely different. This is because of the loss in the microstrip line sections which leads to dramatically change in attenuation level. This graph shows a simulated performance for a microwave component, like a filter or transmission line. The graph shows attenuation (in dB) versus frequency. According to m1, at 2.0 GHz frequency, the insertion loss of the component is -3.912 dB. The Insertion loss is -3.088 dB at 7.0 GHz as shown by marker m2. The small change in attenuation with frequency suggests that this component is either broadband or working in its passband since it does not show the large signal rejection of a filter's stopband. The low insertion loss means that through this frequency range the component transmits signals efficiently with little power loss.
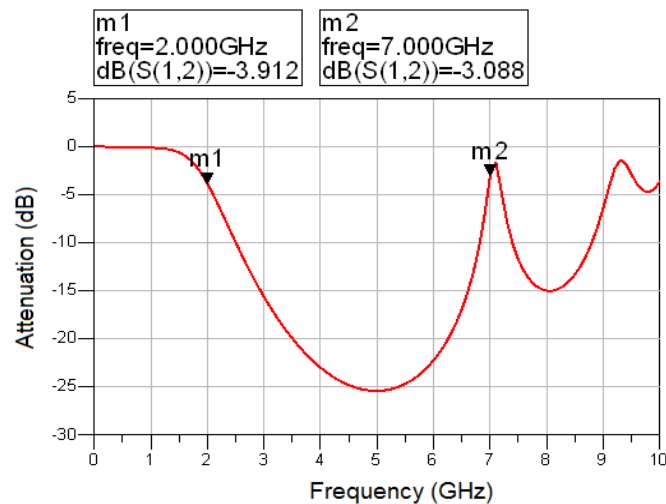

Fig 8. Response of step-impedance LPF

The response of BSF is also investigated and plotted in both disable and magnitude as shown in Figures 9 and 10 respectively. Additionally, this power divider works great, it's likely a Wilkinson Power Divider, as seen on the graphs. Figure 9 describes the transmission coefficient from the input to one output port. The insertion loss of about -3.01 dB is indicated by marker m1 at 3.0 GHz and marker m2 at 7.0 GHz. This value is the ideal theoretical value for receiving two equal power outputs (-3.01 dB). The fact that it stands for 3 GHz to 7 GHz proves that the power divider has an excellent performance and a wide bandwidth because it can divide the power equally and sustained with low loss within the entire band.

Figure 9. Response of lamped element BSF in dB

The graph in Figure 10 includes the value of the S(1,2) transmission coefficient, proves that the power divider performs well. Both markers m3 and m4 measure a magnitude of 0.707. The first one m3 is set at 3.0 GHz and the next m4 is set at 7.0 GHz. This value is no accident. Mathematically, it is equivalent to a -3.01 dB power loss, which occurs in a perfect equal split. With this connection, one of the output ports will have half the voltage (and, therefore, power). This 0.707 value from 3 GHz to 7 GHz shows that the power divider has power division and flat frequency response that is close to ideal over the wide bandwidth.
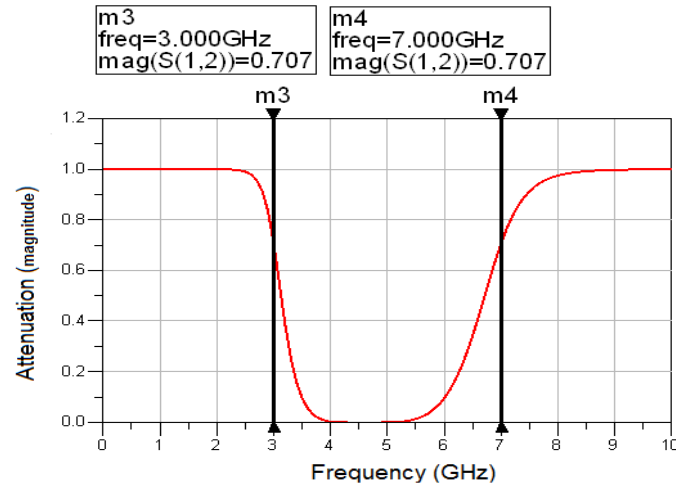

Figure 10. Response of lamped element BSF In magnitude

From BSF corresponding response, it is clear to see that the rejection band is in the frequency range between 3 and 7 GHz as desired.

The comparison of the frequency response characteristics of the two implemented LPF's. The ideal response from a theoretical design of the LC component in Figure 11 (a) is indicated by the blue line (Lumped LPF). Meanwhile, the red dotted line (Microstrip LPF) shows the response from the microstrip device. The two filters meet the design specification by allowing frequencies below the 2 GHz cut-off through and rejecting frequencies above it. The reason the two curves differ, in particular the larger insertion loss and slightly different roll-off of the microstrip version, is because of the conductor and dielectric losses in the physical transmission lines. These losses are not present in the ideal, lumped-element simulation.

The performance of the proposed Band Stop Filter (BSF) is illustrated in this plot in Figure 11 (b). The filter is successfully producing a deep notch/stopband between 3 GHz and 7 GHz as per design specification. Between these alternative ranges, the input signal is severely attenuated or blocked. Outside this stopband, at lower and higher frequencies, the signal passes through with minimum attenuation. The sharpness of the filter response in the stopband edges (3 GHz and 7 GHz) indicates that the filter is efficient at the respective band edges.

The diagram in Figure 11 (c) physically shows the designed microstrip low-pass filter. It displays how the filter would be made on circuit board. The microstrip lines are capacitive, low-impedance lines and are shown in wide-red sections. The inductive, high-impedance lines are shown in narrow-blue sections. The varied length of these sections corresponds to the calculated electrical lengths necessary to simulate the behavior of the lumped capacitors and inductors in the original design. That is, we are implementing an electrical schematic into a physical layout.

The bar graph in Figure 11 (d) offers a tangible, numerical comparative analysis of both LPF implementations at specific frequencies. The first batch of bars (Root@ 7 GHz) indicates that both filters have at least a 50 dB attenuation at the specified stopband. The second bars (IL 1 GHz) compare the insertion loss in the passband, less is better. The tradeoff is clear from the chart: while the lumped-element filter has superior performance (lower loss in passband and greater attenuation in stopband), the microstrip implementation is a practical planar structure with prospect for actual circuits.
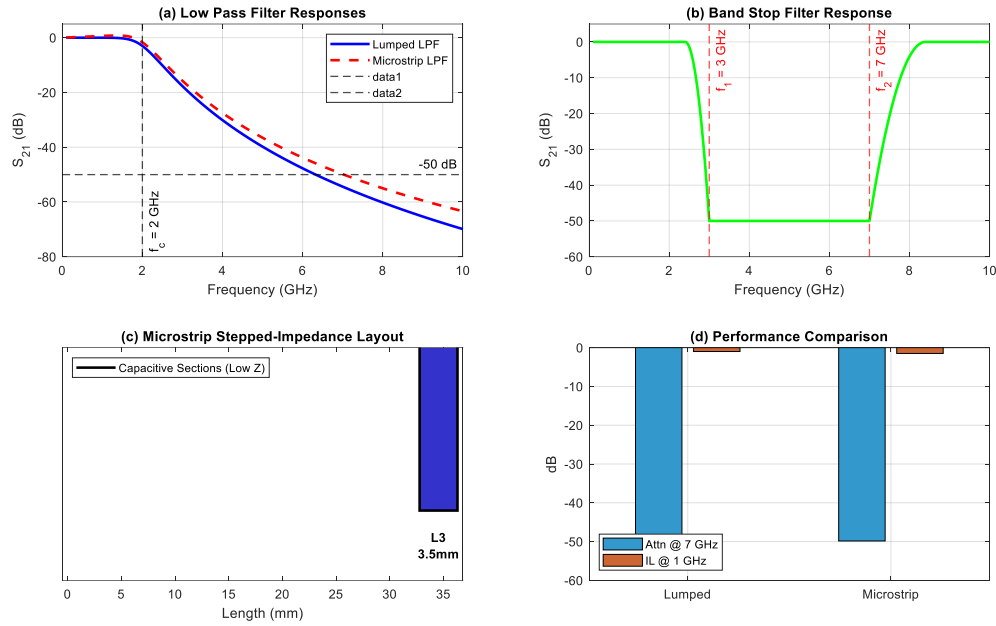
Figure 11: Breakdown results, (a) Low Pass Filter Responses, (b) Band Stop Filter Response, (c) Microstrip Stepped-Impedance Layout, (d) Performance Comparison

Conclusion

The design, simulation, and verification of lumped-element and microstrip stepped-impedance LPF and lumped-element BSF have been successfully detailed in this paper. The respondent used Advanced Design System (ADS) software to realize a Butterworth filter response with a maximally flat configuration. The design procedures are surely validated by the simulation results. Both the lumped and distributed forms of the low-pass filters were able to achieve the cut-off frequency of 2 GHz. The lumped LPF also demonstrates a stopband of 54 dB at 7 GHz, which exceeds the 50 dB requirement. The design of the band-stop filter was accomplished successfully. Simulation results confirm that the stopband is well defined from 3 GHz to 7 GHz. To summaries, every main design objective was met, showing the simulation filter characteristics.

Recommendations for Future Work.

For future research, some directions to build upon the foundation laid in this paper are recommended.

The next step is to go from simulation to experimental testing and validation of the prototype. Making a microstrip stepped-impedance low pass filter on PCB and taking measurement with Vector Network Analyzer (VNA) will allow critical comparisons of the simulated and measured performances. This would highlight how things like production tolerances, differences in substrate materials and connector losses affect the system.

A more detailed comparison might be performed between the two LPF implementations. Future work can be done to quantify insertion loss in the passband, roll-off (transition band) sharpness, and attenuation of the microstrip LPF at 7 GHz. This will clarify the performance trade-offs of ideal lumped components versus practical transmission line structures.

Lumped elements used to design the BSF were used in this work. One big extension would be to design, simulate and fabricate a Band-Stop Filter using microstrip technology, a coupled-line or hairpin filter structure. This would produce a completely planar filter system and would create its own distinctive design challenges and results.

The filters can be optimized for any application requirements that may arise. This might involve miniaturizing the microstrip layout by meandering, improving the stopband rejection, and designing for a steeper roll-off with the Chebyshev response function

References

[1] R. Tüzün and N. Akçam, "Design of Microstrip Low Pass Filters," International Symposium on Innovative Technologies in Engineering and Science, Nov. 2018.

[2] P. Mishra, and M. U. Amin, "Design of a Low pass filters with Chebyshev approximation using Serenade and realization of the low pass filters in microstrip," Journal of Emerging Technologies and Innovative Research, Vol. 6, No. 6, Jun 2019.

[3] S.B. Haddi, A. Zugari, A. Zakriti and S. Achraou, "Design of a Band-Stop Planer Filter for Telecommunications Applications ,". 13th International Conference Interdisciplinarity in Engineering, 2019, pp. 788-792.

[4] Amini, B., Rastegar, H., & Pichan, M. (2024). An optimized proportional resonant current controller based genetic algorithm for enhancing shunt active power filter performance. International Journal of Electrical Power & Energy Systems, 156, 109738. https://doi.org/10.1016/j.ijepes.2023.109738

[5] Cao, X., Su, X., Yang, P., Gao, Y., Wu, D. O., & Quek, T. Q. S. (2025). Survey on Near-Space Information Networks: Channel Modeling, Transmission, and Networking Perspectives. IEEE Communications Surveys & Tutorials, 1–1. https://doi.org/10.1109/COMST.2025.3549523

[6] Dobrev, D., Neycheva, T., Krasteva, V., & Jekova, I. (2025). Design of High-Pass and Low-Pass Active Inverse Filters to Compensate for Distortions in RC-Filtered Electrocardiograms. Technologies, 13(4), 159. https://doi.org/10.3390/technologies13040159

[7] Li, Z., Xue, W., Xu, Q., Wu, H., & Chen, M. (2025). Synchronicity and energy evolution of field-coupled Chua's circuits via parallel inductor-capacitor coupling channel. Chaos, Solitons & Fractals, 197, 116545. https://doi.org/10.1016/j.chaos.2025.116545

[8] Liu, Y., Zhou, J., Li, C., Zhang, H., Wang, Y., Yan, Y., Duan, L., Cheng, Z., Ma, Y., & Yao, Z. (2025). Interfacial coupling effects in two-dimensional ordered arrays for microwave attenuation. Nature Communications, 16(1), 202. https://doi.org/10.1038/s41467-024-55776-9

[9] Modaberi, S. A., Bolandi, T. G., Hassanifar, M., & Neyshabouri, Y. (2025). A high step-up single switch DC-DC quadratic boost converter based on coupled inductor with reduced voltage stress of power components. International Journal of Circuit Theory and Applications, 53(5), 2691–2717. https://doi.org/10.1002/cta.4233

[10] Romero, M. C., Reyes-Ayala, M., Andrade-Gonzalez, E. A., Chavez-Sanchez, S., Terres-Peña, H., Salgado-Guzman, G., & Rodriguez-Rivera, R. (2025). Algorithm to Calculate PCB Stepped-Impedance Low-Pass Filters for Microwave Applications. WSEAS TRANSACTIONS ON COMMUNICATIONS, 24, 17–22. https://doi.org/10.37394/23204.2025.24.4

[11] Selvaprasanth, P., Karthick, R., Meenalochini, P., & Prabaharan, A. M. (2025). FPGA implementation of hybrid Namib beetle and battle royale optimization algorithm fostered linear phase finite impulse response filter design. Analog Integrated Circuits and Signal Processing, 123(2), 33. https://doi.org/10.1007/s10470-025-02385-1

[12] Wu, H., Wu, B., Meng, X., Bao, Q., Wang, W., Ye, L., & Sun, X. (2024). Enhanced Imbalance-Distortion Mitigation and Noise Suppression in I / Q -Based Phase Demodulation Systems. IEEE Sensors Journal, 24(9), 14413–14427. https://doi.org/10.1109/JSEN.2024.3374811

[13] Xiao, B., Zhu, W., Lin, H., Yu, J., Mi, H., & Xiao, L. (2025). A reconfigurable multi-passband multifunctional device for wireless communications based on spoof surface plasmon polaritons. Physica Scripta, 100(8), 085501. https://doi.org/10.1088/1402-4896/adf01d

[14] Zhang, Y., Dong, H., Chen, J., Wang, M., Zhang, L., Zeng, Z., Li, H., Zhang, Z., & Liu, Y. (2025). Automatically starting, flat-top electro-optic frequency comb based on photonic sampling. Optics Letters, 50(23), 7231. https://doi.org/10.1364/OL.577991